Brain Pathology ISSN 1015–6305

RESEARCH ARTICLE

Upregulation of cystathione β-synthase and p70S6K/S6 in neonatal hypoxic ischemic brain injury

Mirna Lechpammer[1], Yen P. Tran[1], Pia Wintermark[2], Veronica Martínez-Cerdeño[1,3,4], Viswanathan V. Krishnan[1], Waseem Ahmed[1], Robert F. Berman[3,5], Frances E. Jensen[6], Evgeny Nudler[7], David Zagzag[8]

[1] Department of Pathology and Laboratory Medicine, University of California Davis, Sacramento, CA.
[2] Department of Pediatrics, Division of Newborn Medicine, Montréal Children's Hospital, McGill University, Montréal, QC, Canada.
[3] MIND Institute, University of California Davis, Sacramento, CA.
[4] Institute for Pediatric Regenerative Medicine and Shriners Hospital for Children of Northern California, Sacramento, CA.
[5] Department of Neurological Surgery, University of California Davis, Sacramento, CA.
[6] Department of Neurology, University of Pennsylvania, Philadelphia, PA.
[7] Howard Hughes Medical Institute and Department of Biochemistry, New York University School of Medicine, New York, NY.
[8] Departments of Pathology and Neurosurgery, Division of Neuropathology, Microvascular and Molecular Neuro-Oncology Laboratory, Perlmutter Cancer Center, New York University Langone Medical Center, New York, NY.

Keywords
autism, brain injury, CBS, hypoxia, mTOR, prematurity.

Corresponding author:
Mirna Lechpammer, MD, Ph.D., Assistant Professor, Neuropathology, Department of Pathology and Laboratory Medicine, University of California Davis, 4400 V Street, PATH Building, Room 1227, Sacramento, CA 95817 (E-mail: *mlechpammer@ucdavis.edu*)

Received 19 April 2016
Accepted 12 July 2016
Published Online Article Accepted 28 July 2016

doi:10.1111/bpa.12421

ABSTRACT

Encephalopathy of prematurity (EOP) is a complex form of cerebral injury that occurs in the setting of hypoxia-ischemia (HI) in premature infants. Using a rat model of EOP, we investigated whether neonatal HI of the brain may alter the expression of cystathionine β-synthase (CBS) and the components of the mammalian target of rapamycin (mTOR) signaling. We performed unilateral carotid ligation and induced HI (UCL/HI) in Long-Evans rats at P6 and found increased CBS expression in white matter (i.e. corpus callosum, cingulum bundle and external capsule) as early as 24 h (P7) postprocedure. CBS remained elevated through P21, and, to a lesser extent, at P40. The mTOR downstream target 70 kDa ribosomal protein S6 kinase (p70S6K and phospho-p70S6K) and 40S ribosomal protein S6 (S6 and phospho-S6) were also overexpressed at the same time points in the UCL/HI rats compared to healthy controls. Overexpression of mTOR components was not observed in rats treated with the mTOR inhibitor everolimus. Behavioral assays performed on young rats (postnatal day 35–37) following UCL/HI at P6 indicated impaired preference for social novelty, a behavior relevant to autism spectrum disorder, and hyperactivity. Everolimus restored behavioral patterns to those observed in healthy controls. A gait analysis has shown that motor deficits in the hind paws of UCL/HI rats were also significantly reduced by everolimus. Our results suggest that neonatal HI brain injury may inflict long-term damage by upregulation of CBS and mTOR signaling. We propose this cascade as a possible new molecular target for EOP—a still untreatable cause of autism, hyperactivity and cerebral palsy.

INTRODUCTION

Encephalopathy of prematurity (EOP) is a form of brain injury caused by either primary or secondary hypoxia-ischemia (HI) that occurs during the premature or complicated delivery (30). EOP has enormous healthcare implications as annually 1.5% of all newborns in the USA are born with a very low birth-weight (≤1500 g) and 25–50% of them subsequently exhibit elements of autism spectrum disorder (ASD) (8, 30). Cognitive, behavioral, attention, or socialization deficits and hyperactivity are combined in 5–10% of affected infants with various degrees of motor deficits and cerebral palsy (7). Thus, surviving children typically require medical care well into their adolescence and sometimes for the rest of their lives (30).

While the mechanisms of neonatal HI brain injury are multifactorial, several studies have strongly suggested that endogenous hydrogen sulfide (H_2S) acts as a mediator of cerebral ischemic damage following oxygen deprivation (22, 33). H_2S is regarded, along with nitric oxide and carbon monoxide, as a gaseous neurotransmitter and endogenous neuromodulator that plays multiple roles in the central nervous system under physiological and pathological conditions, especially in secondary neuronal injury (5, 31). The precursor of H_2S, cysteine (Cys), is innocuous under normal conditions, but causes toxicity in neurons that are deprived of glucose, oxygen, or both (33). Elevated extracellular levels of Cys have been found *in vivo* in animals with ischemic brain injury caused by carotid artery ligation (26). High plasma Cys levels are

associated with poor clinical outcome in patients with the acute stroke (33). The increased conversion of Cys to H_2S by cystathionine β-synthase (CBS) appears to be an important contributor (mechanism) to the pathophysiology of HI-induced brain injury.

Animal models of cerebral reperfusion injury have demonstrated that H_2S antagonists ameliorate its associated injury, inflammation and circulatory shock (19, 27). In addition, a recent report has identified inhibition of synthesis of H_2S as a likely mechanism by which electro-acupuncture exerts neuroprotective effects in a rat model of HI brain injury (18). H_2S has been shown to act via cAMP-mediated phosphatidylinositol 3-kinase (PI3K)/Akt/mTOR signal transduction pathways (25). The mammalian target of the rapamycin pathway (mTOR), may contribute to the establishment of synaptic connections in developing neurons, as excessive mTOR signaling is implicated in abnormal neuronal and glial development and gross brain malformations (28). Our group has recently demonstrated that two components of the mTOR signaling cascade, 70 kDa ribosomal protein S6 kinase (p70S6K) and 40S ribosomal protein S6, are overexpressed in neonatal brain tissue of infants with EOP during gestational weeks 36–39 (16). The S6 kinase p70S6K is positioned downstream of PI3K/Akt/mTOR pathway, and is activated by 3-phosphoinositide-dependant protein kinase 1 and mTOR (25, 28). In turn, p70S6K activates 40S ribosomal protein S6, which causes an increased rate of translation of the class of 5′ terminal oligopyrimidine mRNA transcripts, thus regulating protein synthesis (25, 28).

In this study, in order to provide molecular validation of results seen in premature infants with neonatal HI brain injury (16), we investigated whether hypoxia-ischemia alters the expression of CBS and the components of the mTOR signaling pathway in the rat model of EOP. In particular, we examined manipulation of components of the mTOR pathway as a therapeutic strategy in EOP by blocking the mTOR pathway directly with the small-molecule inhibitor everolimus (6).

MATERIALS AND METHODS

Animal model of EOP

White matter injury was produced in P6 Long-Evans rat pups by unilateral carotid artery ligation (UCL) followed by severe hypoxia (6% O_2 for 1 h), as previously described (15). In brief, rats were anesthetized (isoflurane; 2.5–5% for induction and 1–4% for maintenance) and unilaterally the proximal internal carotid artery was isolated from the sympathetic chain and clamped. Animals were placed on a thermal blanket for the remainder of the HI procedures to maintain body temperature between 33 and 34°C. After a 1 h recovery, the rats were placed in a sealed chamber infused with nitrogen to achieve an O_2 level of 6% for 1 h. To examine the cell specificity of injury and time the course of changes in the expression of mTOR signaling molecules, rats were sacrificed at 24 h (P7), 4 days (P10), 8 days (P14), 15 days (P21) or 34 days (P40) after UCL/HI and compared to healthy normoxic controls or animals treated with everolimus. Briefly, animals were deeply anesthetized with sodium pentobarbital and transcardially perfused. Brains were extracted, postfixed overnight in 4% paraformaldehyde and then cryoprotected in 30% sucrose. For Western blot analyses, rats were decapitated and brains rapidly removed. Brains were placed on a precooled dissecting block and white matter consisting of corpus callosum, cingulum bundle and external capsule was rapidly dissected via micropunch. Histological, immunofluorescence and Western blot analyses were carried out for CBS, S6 and phospho-S6, p70S6K and phospho-p70S6K. All procedures were performed in accordance with the guidelines of the UC Davis Animal Use and Care Committee.

Treatment regimens and design

Experimental animals were treated with everolimus (also known as RAD001) solely *after* severe HI brain injury, thus closely mimicking clinical events in EOP. Everolimus was given by oral gavage at a dose of 10 mg/kg or vehicle twice per day for 3 or 5 days starting 12 h after UCL/HI.

Histological brain tissue analysis and immunofluorescent methods

For all experimental rats, stereotaxic coordinates were used as follows: for P7, P10 and P14, 2.8–3.1 mm from bregma, 2.6–3.0 mm lateral to midline; for P21 and P40, 3.0–3.4 mm from bregma, 2.4–3.4 mm lateral to midline. Serial 20 μm coronal sections were cut by cryostat from the anterior extent of the lateral ventricles through the posterior extent of the dorsal hippocampus. Coronal sections at the level of the middorsal hippocampus were examined. Representative sections of parietal cortex and white matter were stained by hematoxylin and eosin (H&E) and/or immunofluorescent labeling, as previously published (12, 15, 16). To avoid experimenter bias, two neuropathologists (ML and DZ) performed all histological and immunofluorescent evaluations in a blinded fashion and agreed on the final scoring.

Antibodies

The following antibodies have been used for immunofluorescence procedures: (1) an anti-CBS rabbit polyclonal Ab (Cat. No., ab96252, 1:200, Abcam, Cambridge, MA); (2) an anti-phospho-S6 ribosomal protein ($Ser^{240/244}$) rabbit polyclonal antibody (Cat. No. 2215, 1:200, Cell Signaling, Boston, MA); (3) an anti-GFAP mouse monoclonal antibody (Cat No. 3670S, 1:250, Cell Signaling, Boston, MA); (4) an anti-OLIG2 mouse monoclonal antibody (MABN50, 1:100, EMD Millipore, Billerica, MA); (5) an anti-CD68 mouse monoclonal antibody (MCA341GA, 1:400 AbD Serotec, Raleigh, NC); (6) an anti-NeuN mouse monoclonal antibody (MAB377, 1:200, EMD Millipore, Billerica, MA) and anti CD31 mouse monoclonal antibody (M0823, prediluted, Dako, An Agilent Technologies, Carpinteria, CA).

Western blot analyses

Microdissected brain tissue (corpus callosum, frontoparietal lobe) was homogenized (total n = 6–15/group), sonicated, centrifuged and proteins quantified using a Bradford protein assay (BioRad, Berkeley, CA). Thirty micrograms of protein were then equalized and loaded on a 4–20% Tris-glycine gel. After electrophoresis, proteins were transferred to polyvinylidene difluoride membranes, blocked, and incubated with the following antibodies: anti-CBS rabbit polyclonal Ab (Cat. No., ab96252, 1:500, Abcam, Cambridge, MA); mTOR downstream targets anti-p70S6K (Cat. No.

2708, 1:1000, Cell Signaling, Boston, MA), anti-phospho-p70S6K(Thr^{389}) (Cat. No. 9234, 1:1000, Cell Signaling, Boston, MA); anti-S6 (Cat. No. 2217, 1:1000, Cell Signaling, Boston, MA) and anti-phospho-S6 (Ser$^{240/244}$) (Cat. No. 2215, 1:1000, Cell Signaling, Boston, MA), as well as an anti-β-actin mouse monoclonal antibody (A5411, 1:2000, Sigma-Aldrich, St Louis, MO). Blots were imaged on a GE LAS 4000 Image reader and relative optical density for each band was quantified using GE ImageQuant Software and standardized to actin to correct for equal protein loading (Piscataway, NJ). Given that the expression of mTOR components is constitutively higher in a developing brain than in adults, both control and experimental quantifications were defined as a fold increase against baseline mTOR expression in healthy adult rat brains (P65–70, N = 6) (9, 16).

Rat behavioral and locomotor assays

Behavioral and locomotor assays were performed in a blinded fashion regarding previous treatments in young rats (P35–37) following weaning from dams at P21. All naive, sham and UCL/HI animals used for behavioral and locomotor assessments were sacrificed 34 days (P40) post-UCL/HI (P6) and their brains were preserved for protein expression analyses as described above.

Open field locomotion test

This test evaluates exploratory behavior and anxiety in a noninvasive manner. At the beginning of testing, each animal is placed in the center of the open field and monitored during a 30 min test session using the ANY-maze Video Tracking System. Data on distance traveled and time spent in the center and perimeter are automatically calculated by the tracking software (5, 23).

Three-chambered social choice test

Social interactions in rats were assessed using the three-chamber "Social Approach" and "Recognition of Social Novelty" tests adapted from procedures described for mice by Moy *et al* (20). Testing was carried out in a rectangular apparatus made of clear Plexiglas 34.5 × 100 × 100 cm overall (H × W × L), divided into three equal-sized chambers (34.5 × 100 × 33 cm). Circular Plexiglas cages 13.3 cm diameter and 21 cm high, with clear Plexiglas rods spaced 0.5 cm apart, were placed in the two end chambers and used to restrain stimulus rats. A digital camera and a computerized tracking system were used to track the movement of the rat through the apparatus, and to calculate percent of time spent in each of the three chambers (ANY-maze, Stoelting, Wood Dale, IL). For the social approach test, a same sex unfamiliar stimulus rat (i.e. stranger rat) was placed under one of the cages while the other cage remained empty. The test rat was placed into the center chamber and allowed to freely explore the apparatus for 10 min. Untreated rats typically spend more time in the chamber with the caged stimulus rat than in the chamber with the empty cage, and difference is used as an index of sociability. In the preference for social novelty task, the test rat is removed from the apparatus, and an unfamiliar stimulus rat is put under the formerly empty cage, while the now familiar rat is left under its cage. The test rat is returned to the center chamber and allowed to spend time in the chamber with the unfamiliar rat or spend time in the chamber with the earlier, now familiar rat. Untreated rats typically spend more time in the chamber with the new unfamiliar rat compared to the familiar rat, and this difference is used as a measure of preference for social novelty (5, 20).

Automated gait analysis test (CatWalk)

To test the locomotor abilities of rats, we used the Noldus CatWalk XT system to record rat movements within an enclosed walkway (29). The floor of the walkway is a glass plate through which green light is reflected. The pressure of the paw causes scatter of green light, which is recorded by a digital camera. Rats were allowed to traverse the walkway in either direction for the minimum of 10 "compliant" runs. Runs were labeled "compliant" if the run complied with duration interval and speed variation (i.e. animal did not stop along the way or turn around). All runs were captured, however only "compliant" runs were used for analysis. Rats were tested four times following the initial six training runs over 3 days (2, 29).

Statistical analysis

One-way ANOVA and two-tailed *t*-tests were used for multiple comparisons between different experimental (UCL/HI) and control groups. Western blot quantifications were analyzed by Mann-Whitney U test. Statistical significance was defined as $P < 0.05$.

RESULTS

CBS expression is increased in rat white matter following neonatal HI brain injury

We have found by Western blot analysis an increased expression of CBS across white matter regions (i.e. corpus callosum, cingulum bundle and external capsule) of rats as early as 24 h (P7) following UCL/HI at P6 (Figure 1) compared to normoxic controls. This overexpression of CBS further increased in UCL/HI rats relative to controls through 8 days (P14) and reached its peak by 15 days (P21) after the HI brain injury. Interestingly, CBS expression remained elevated at P40 (Figure 1), i.e. 31 days after UCL/HI. Following this pattern, we have also detected by immunofluorescent analysis an increased expression of CBS in astrocytes (GFAP+) in white matter (corpus callosum, cingulum bundle and external capsule) of rats at P10 following UCL/HI at P6 (Figure 2A). H&E staining did not reveal focal lesions or other abnormalities. At the same time, anti-CBS antibodies did not stain neurons (NEUN+) or resting and activated microglia (CD68+), consistent with expression pattern of CBS restricted to astrocytes in brain tissue (Figure 2A) (3).

In order to provide some molecular target validation of the reported proangiogenic effect of H_2S under hypoxic stress (17), we have performed fluorescent double labeling of CBS with endothelial cells (CD31+) in intraparenchymal brain blood vessels in white matter of UCL/HI rats at P10 compared to normoxic controls. The analysis has confirmed both an elevated expression of CBS in intraparenchymal brain blood vessels of UCL/HI rats at P10 relative to normoxic controls, as well as its colocalization with endothelial cells (CD31+) (Figure 2B).

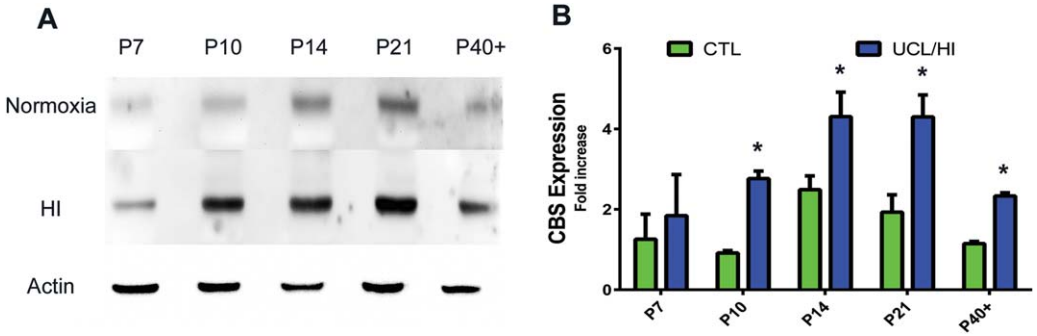

Figure 1. Western blot analysis of CBS expression in the rat brain following UCL/HI at P6 and during normal development. **A.** Representative western blot analyses for CBS at five different developmental time points in UCL/HI animals and age and sex matched normoxic controls. **B.** Western blots quantification of total CBS expression during the same gestational period (n = 8). Histograms represent averaged optical density normalized to actin, and expressed relative to the mean controls values (n = 8). $*P < 0.05$ vs. normoxic controls.

Expression of mTOR downstream targets is increased in rat cortex and white matter following neonatal HI brain injury

Immunofluorescent analysis for phospho-S6 expression yielded markedly elevated staining in neurons of rats at P10 following UCL/HI at P6 compared to normoxic controls (Figure 3). Anti-phospho-S6 antibodies did not stain astrocytes (GFAP+) or oligodendrocytes (OLIG2+) in UCL/HI rats nor normoxic controls (Figure 3). Interestingly, while phospho-S6 did not coexpress on resting and activated microglia (CD68+) in the brain of normoxic rats at P10, such coexpression was detected in UCL/HI rats (Figure 3).

These findings were corroborated by Western blot analyses. Specifically, an increased expression was detected in cortex and white matter of the mTOR downstream targets—p70S6K and phospho-p70S6K (Figure 4A) & S6 and phospho-S6 (Figure 4B,C) as early as 24 h (P7) following UCL/HI at P6 compared to normoxic controls. Overexpression of mTOR components further increased relative to normoxic controls through P14 and continued to be overexpressed in HI rats at P21 and P40 (Figure 4) in a pattern similar to that seen for CBS expression.

Everolimus inhibits expression of mTOR components in the rat model of EOP

Separate cohorts of animals (n = 8) were treated with everolimus (RAD001) for 3 (P10) and 7 days (P14) after UCL/HI at P6 as described in Materials and Methods. At both durations of treatment, a significant inhibition of phospho-S6 expression was observed compared to UCL/HI animals without the treatment (Figure 5), in keeping with the expected pharmacological effect of everolimus in the brain (5). At the applied doses and durations of treatment, everolimus was well tolerated. Individual weight variations between the animals did not exceed the allowable threshold of ±20% (21) in any experimental group. Likewise, the postsurgery mortality did not differ between UCL/HI animals regardless of everolimus or vehicle administration.

mTOR blockade by everolimus reverses/prevents hyperactivity and autism-like behavior in the rat model of EOP

Locomotor behaviors were examined in young rats (P35–37) exposed to UCL/HI at P6 and compared to normoxic control rats. Rats exposed to UCL/HI (n = 13) exhibited significantly less time spent in the perimeter of the open field (Figure 6A; $P = 0.03$) and significantly more entrances into the center zone (Figure 6B; $P = 0.03$) compared with normoxic controls treated with vehicle or everolimus (n = 10/group). Such results indicate hyperactive exploratory behavior and low anxiety levels in UCL/HI rats. As shown in Figure 6, treatment of UCL/HI rats with everolimus (n = 15) has increased time in the field perimeter (Figure 6A) and decreased time spent in the center zone (Figure 6B), thus appearing to normalize locomotor behavior.

When the same UCL/HI and normoxic rats, with and without treatment with everolimus, were tested for sociability in the three-chamber social approach test, both groups showed a significant preference for sociability ($P < 0.0001$), as indicated by greater time spent with a social stimulus (stranger rat) than a nonsocial object (empty wire cage) (Figure 6C). In contrast, in the preference for social novelty test, the preference for interacting with a novel rat over a familiar rat was significantly reduced ($P < 0.0001$) in UCL/HI rats (n = 13) compared with the normoxic controls (n = 10; Figure 6D). Importantly, UCL/HI rats that had been treated with everolimus (n = 15) showed a preference for social novelty that did not differ from normoxic controls (Figure 6D).

mTOR blockade by everolimus (RAD001) reduces motor deficits in the rat model of EOP

Gait analysis, performed by the CatWalk system (P19–20), showed a significant left side-right side asymmetry in the hind limbs pawprint mean contact intensity (Figure 7A; $P = 0.0009$) and maximum contact area (Figure 7B; $P < 0.0001$) in UCL/HI animals (n = 13) compared to normoxic controls treated with everolimus (n = 10). Treatment of UCL/HI rats with everolimus (n = 15) has normalized the hind limbs pawprint mean contact intensity and left side – right side asymmetry observed in untreated animals was lost ($P = 0.115$). Although the similar trend was also observed for the pawprint maximum contact area, a subtle left side-right side difference was still observed in everolimus treated animals (Figure 7B; $P < 0.05$).

DISCUSSION

Results presented here demonstrate an increased expression of CBS in the white matter of rats as early as 24 h (P7) following HI brain

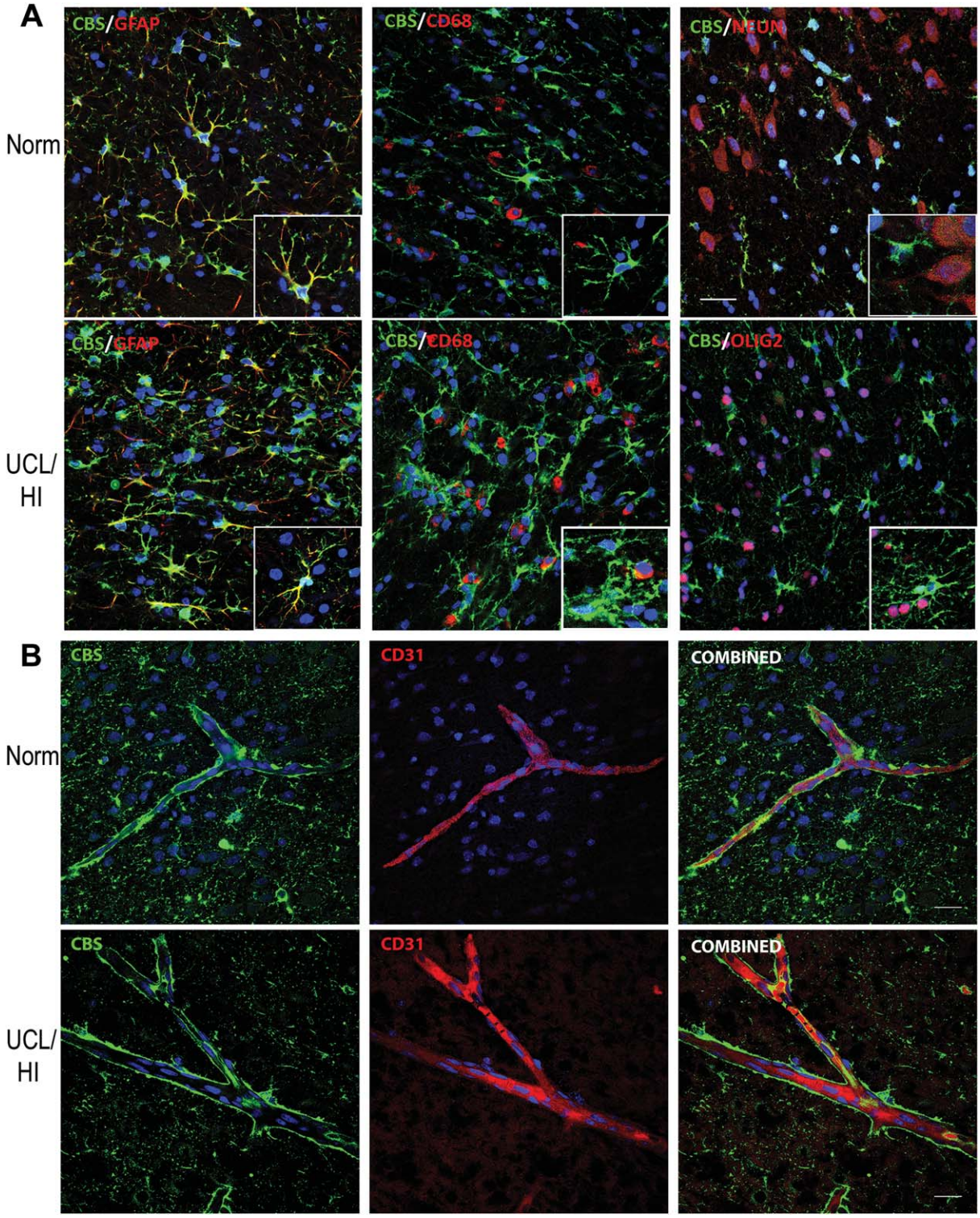

Figure 2. Immunohistochemical analysis of CBS expression in the rat brain at P10 following UCL/HI at P6 compared to normoxic controls. **A.** Representative immunohistochemical stains showing increased expression of CBS in astrocytes (GFAP+) in white matter (interface of corpus callosum and cingulum bundle) of rats at P10 following UCL/HI at P6 compared to normoxic controls (Norm). No CBS coexpression was detected with double labeling for resting and activated microglia (CD68+) or neurons (NEUN+) (*size bar 50* μ*m*). **B.** Representative immunohistochemical stains showing slightly elevated expression of CBS in intraparenchymal brain blood vessels in brains of UCL/HI rats at P10 compared to normoxic controls (Norm) with colocalization of CBS on double staining for endothelial cells (CD31+) (*size bar 50* μ*m*).

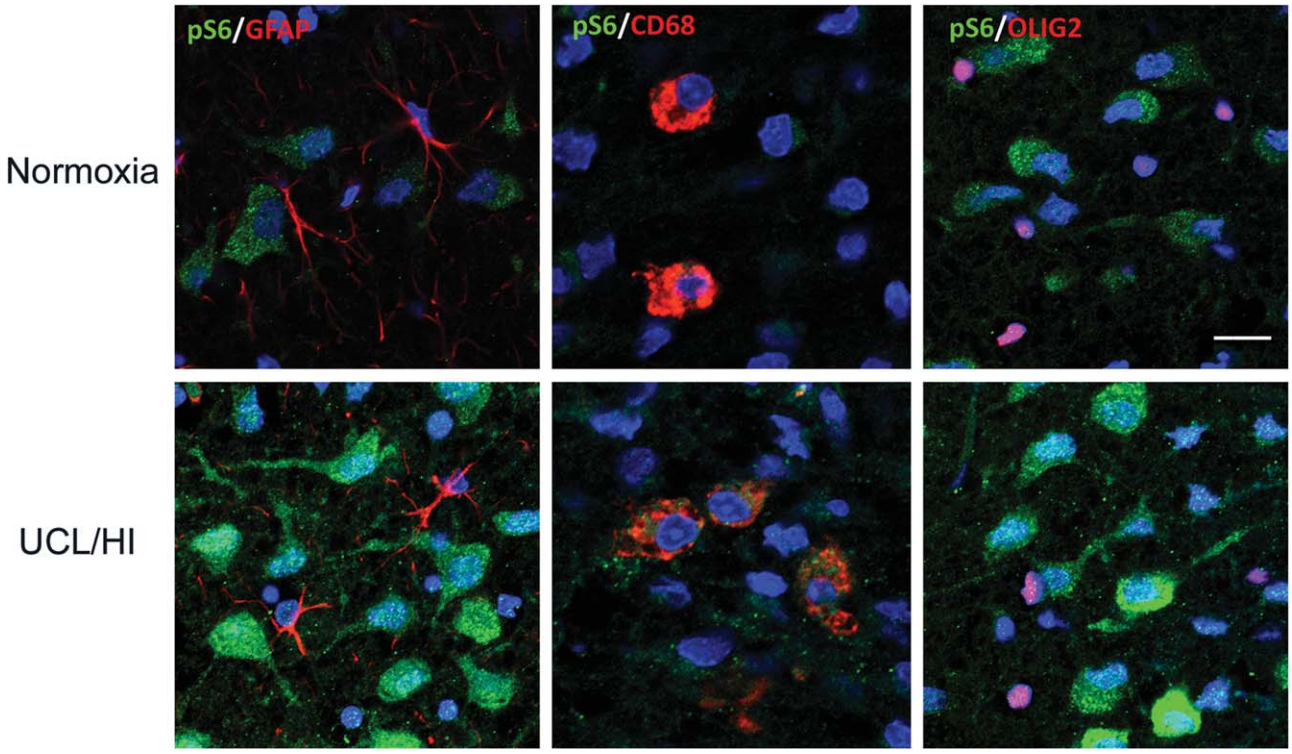

Figure 3. Immunohistochemical analysis of phospho-S6 expression in the rat brain at P10 following UCL/HI at P6 compared to normoxic controls. Representative immunohistochemical stains of deep cortical layers of parietal lobe showing increased phospho-S6 (pS6) expression in neurons of rats 4 days after UCL/HI compared to age and sex matched normoxic controls. There is no pS6 coexpression on astrocytes (GFAP+) or oligodendrocytes (OLIG2+) in neither UCL/HI rats nor normoxic controls. pS6 coexpression is visible on double staining for resting and activated microglia (CD68+) in UCL/HI rats, but not normoxic controls (*bar size 50* μ*m*).

injury (UCL/HI) at P6. Expression of CBS remained elevated 15 days (P21) after the HI insult, and to a lesser extent in young rats (P40), 31 days after UCL/HI. CBS has been implicated as the predominant enzyme in the brain responsible for synthesis of *endogenous* H_2S, an important mediator of cerebral ischemic damage following oxygen deprivation (22, 33). Our results thus also suggest, albeit circumstantially, presumptively higher H_2S concentrations in the rat brain following HI insult. Physiological concentrations of H_2S enhance the N-methyl-D-aspartate (NMDA) glutamate receptor function through activation of adenylyl cyclase (13). Increased production of cAMP, observed in primary cultures of both neuronal and glial cells, results in phosphorylation of NMDA receptor subunits at specific sites by protein kinase A. This in turn activates NMDA receptor-mediated excitatory responses

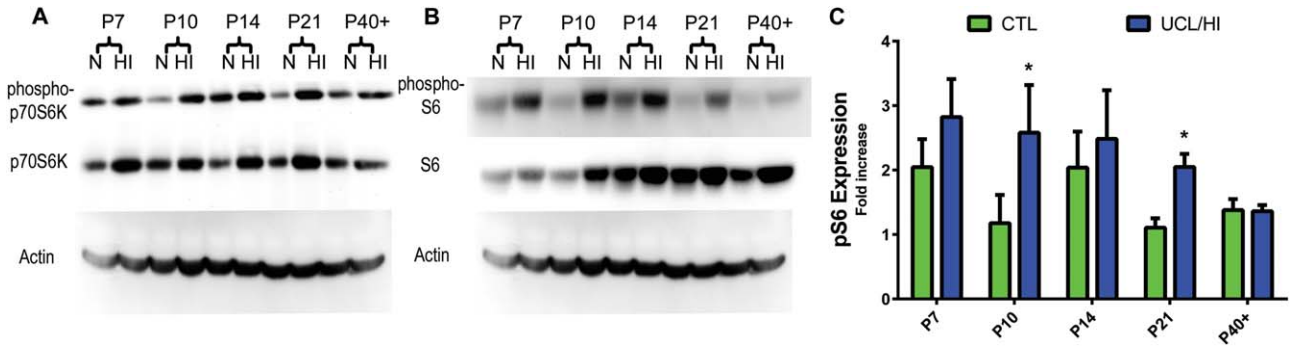

Figure 4. Expression of components of the mTOR signaling cascade in the rat brain following UCL/HI at P6 and during normal development. Representative Western blot analysis of (**A**) mTOR downstream targets phospho-p70S6K & p70S6K and (**B**) phospho-S6 and S6 at five different developmental time points in UCL/HI animals (HI) and age and sex matched normoxic controls (N). (**C**) Western blots quantification of phospho-S6 (pS6) expression during the same gestational period (n = 8). Histograms represent averaged optical density normalized to actin, and expressed relative to the mean controls values (n = 8). $*P < 0.05$ vs. normoxic controls.

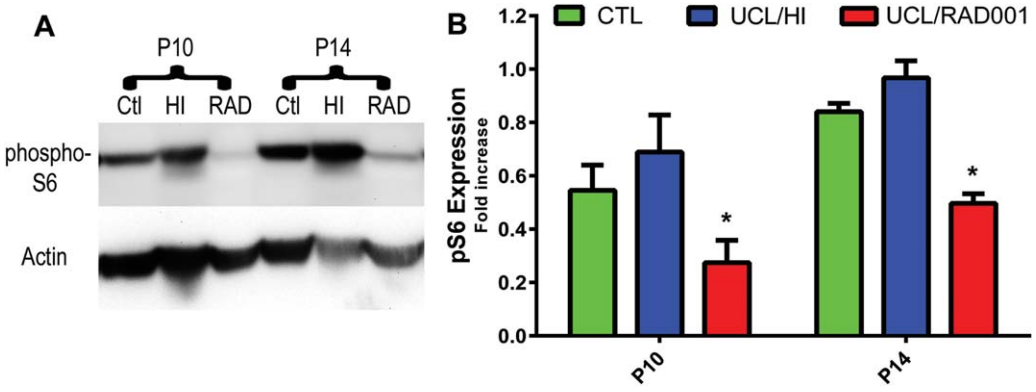

Figure 5. Everolimus reduces expression of phospho-S6 after 3 and 7 days of treatment following UCL/HI at P6. **A.** Representative Western blot analyses of phospho-S6 in UCL/HI rats treated for 3 (P10) and 7 (P14) days with everolimus (RAD) compared to untreated animals (HI) and normoxic controls (Ctl). **B.** Western blots quantification of phospho-S6 (pS6) expression for both treatment periods (n = 8). Histograms represent averaged optical density normalized to actin, and expressed relative to the mean controls values (n = 8). *$P < 0.05$ UCL/HI rats treated with everolimus vs. untreated UCL/HI animals.

including induction of long-term potentiation (LTP) (13). Thus, in cerebral ischemia, H_2S may effectively enhance the NMDA receptor mediated glutamate excitotoxicity, leading to delayed neuronal death due to inflammation, oxidative stress and apoptosis. H_2S has been previously reported to exert its activity in brain through the PI3K/Akt/mTOR signaling pathway (25). mTOR function is influenced by the activities of neuronal surface receptors and channels including NMDA receptors, and dopaminergic and metabotropic glutamate receptors (mGluRs), which are vital for the induction and maintenance of the long-term potentiation and depression (LTP and LTD) of excitatory synaptic transmission (9, 11). mTOR couples these receptors to the transduction mechanisms

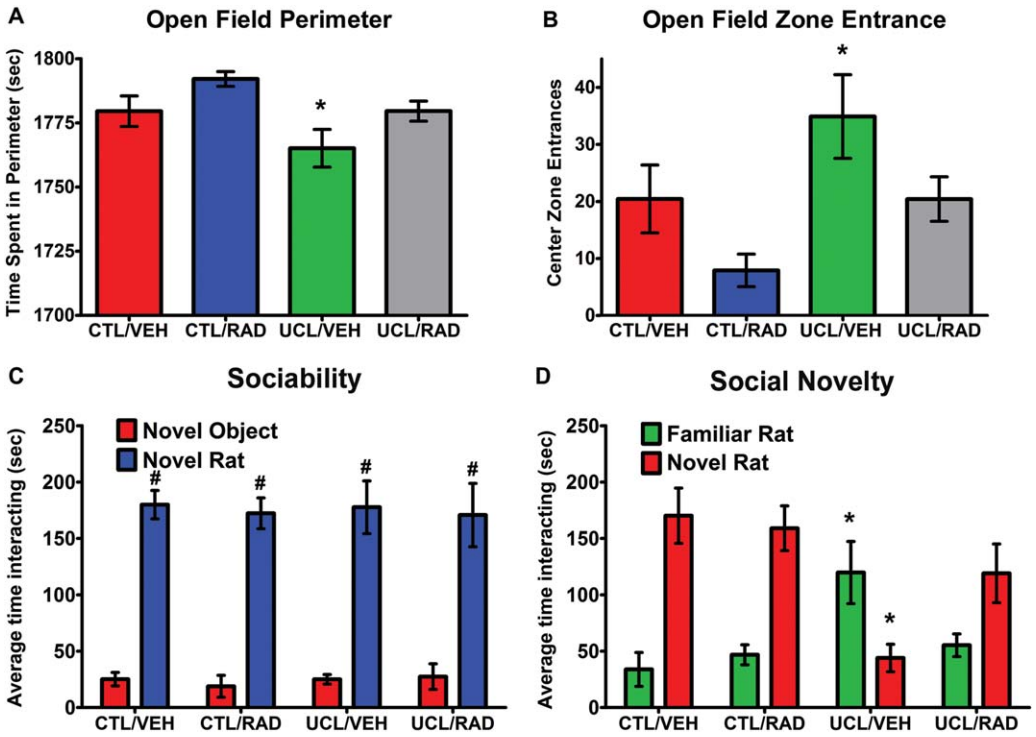

Figure 6. Behavioral assessment for hyperactivity and autism like behavior of young rats exposed to UCL/HI at P6. Experimental groups were prepared and submitted to behavioral assessments as described in Materials and Methods. Depicted are behavioral patterns as assessed by (**A**) open field perimeter; (**B**) open field zone entrance; (**C**) sociability and (**D**) social novelty in P35–37 rats exposed to UCL/HI at P6 and treated with vehicle (UCL/VEH; $n = 13$) or everolimus (UCL/RAD; $n = 15$) compared to normoxic controls treated with vehicle (CTL/VEH; n = 10) or everolimus (CTL/RAD; $n = 10$). #$P < 0.05$ vs. nonsocial object (novel object); *$P < 0.05$ vs. normoxic controls.

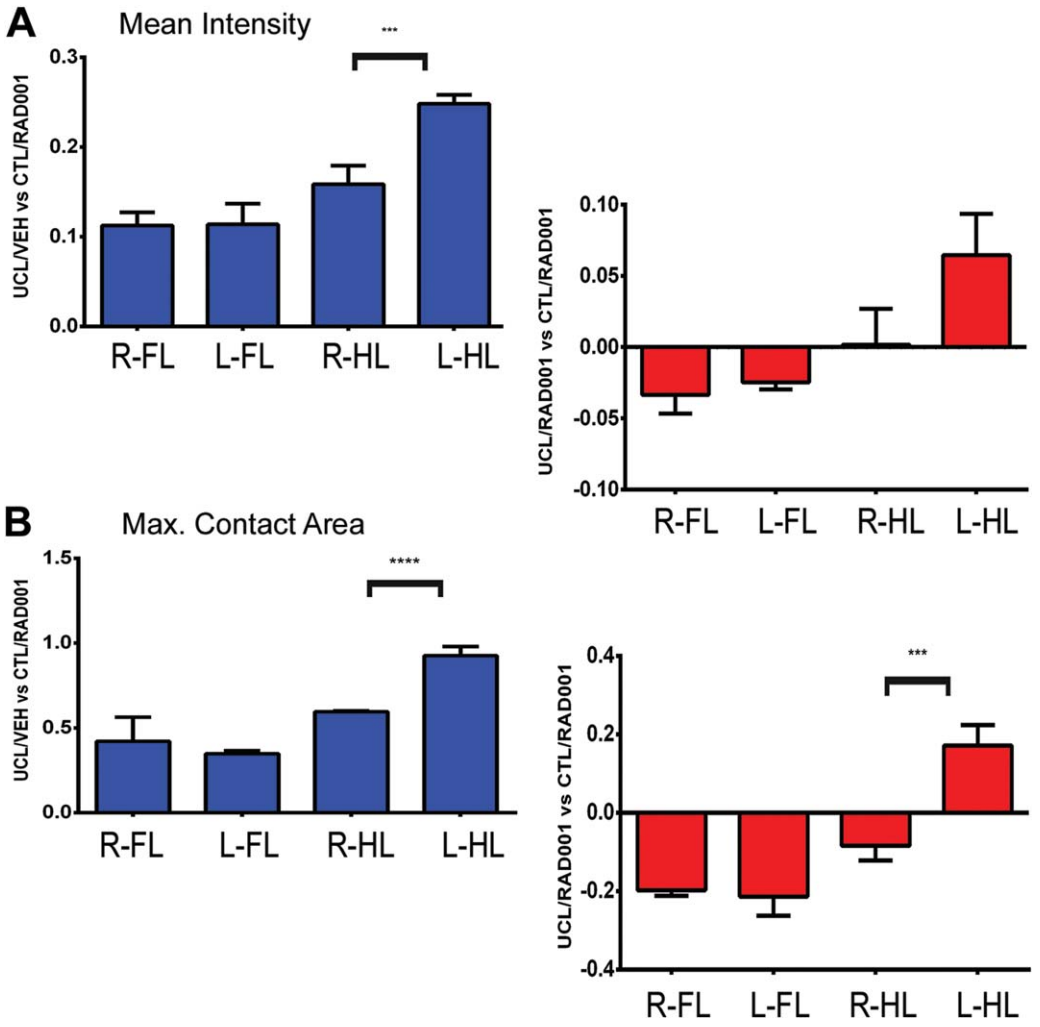

Figure 7. Catwalk automated gait analysis of young rats exposed to UCL/HI at P6. Experimental groups were prepared and submitted to catwalk gait analysis as described in Materials and Methods. Depicted are mean ratios (±SEM) of pawprints mean contact intensity (**A**) and maximum contact area (**B**) for right (R) and left (L) forelimbs (FL) and hindlimbs (HL) of P35–37 rats exposed to UCL/HI at P6, normalized against age and sex matched normoxic controls (treated with everolimus, CTL/RAD; n = 10). Right side/left side gait analysis is shown for UCL/HI rats treated with vehicle (UCL/VEH; n = 13) or everolimus (UCL/RAD; n = 15). $*P < 0.05$ right vs. left side.

responsible for establishing long-lasting synaptic changes that are thought to be the basis for higher order brain functions, including long-term memory (9).

In our study, expression of all tested mTOR downstream targets (p70S6K and phospho-p70S6K & S6 and phospho-S6) was increased at the same time points as observed for the increased expression of CBS in the UCL/HI rats compared to normoxic controls. Such enhanced activation of the mTOR signaling pathway in UCL/HI rats closely resembles the patterns of expression of mTOR signaling molecules recently reported by our group in premature infants with EOP (16). In the same study we also showed coexpression of mGluR5 with phospho-S6 on neurons of EOP patients during gestational weeks 36–39 (16). Therefore, based on our novel results presented here and on previously published data, perturbation of the mTOR signaling cascade appears to be a common pathophysiological feature of several human neurological disorders, including inherited syndromes of cognitive disability and ASD, as well as EOP (9, 16).

Under hypoxic conditions, activation of mTOR potently enhances the activity of hypoxia-inducible factor-1α (HIF-1α) and vascular endothelial growth factor (VEGF) secretion thus increasing angiogenesis, which is reversed with rapamycin (14). Intriguingly, Azmitia at al. recently reported evidence of persistent angiogenesis in postmortem brains from ASD patients but not control brains (1). Our results indicate an overexpression and colocalization of CBS on the endothelial cells (CD31+) in the intraparenchymal brain blood vessels of UCL/HI rats at P10 relative to normoxic controls. This localization is consistent with the previously reported role of H_2S in the upregulation of HIF-1α and VEGF protein levels and an increased HIF-1 binding activity in the rat brain under hypoxic condition (17). The same authors have suggested involvement of HIF-1α/VEGF signaling in the H_2S promoted proliferation and migration of endothelial cells (17). In addition, our

group recently reported VEGF expression in the brain of an asphyxiated newborn treated with hypothermia in the first days of life and of rat pups 24–48 h after the HI injury, including an increased endothelial cell count in the cortex of rat pups 7 and 11 days after HI (24). Thus, while the link between neonatal HI brain injury, mTOR and angiogenesis is emerging (17, 24, 34), the full role of H_2S in this process is yet to be elucidated and warrants further studies.

Given that there are no clinically applicable inhibitors of H_2S synthesis (or CBS, for that matter), in this study we have explored a novel therapeutic strategy in EOP by blocking mTOR with everolimus, an FDA approved drug for treatment of tuberous sclerosis associated subependymal giant cell astrocytoma (6, 10). At the molecular level, administration of everolimus *after* UCL/HI blocked expression of phospho-S6 with approximately comparable efficacy after both 3 days (P10) and 7 days (P14) of treatment, mimicking clinical events in EOP that favor postinsult initiation of treatment. Open field locomotion test performed in young animals (P35–37) exposed to UCL/HI at P6 indicated hyperactive exploratory behavior and low anxiety levels compared to normoxic controls. At the same time, social behavior assessed by the three-chambered social choice test showed abnormal social behaviors in UCL/HI rats compared to healthy normoxic controls, indicating that early life hypoxic-ischemic injury can impair later social behavior to an extent similar to other models of autism (5, 20). Preserved sociability with lack of normal preference for social novelty in UCL/HI rats could be relevant to the preference of autistic individuals to remain with familiar individuals (5). In the context of our behavioral results it is worthwhile to point out that, although anxiety is not considered a phenomenological characteristic of ASD, problems with anxiety appear more frequently in youth with ASD than in other clinical populations (32). The presentation of anxiety is likely affected by age, level of cognitive functioning and degree of social impairment (32). Furthermore, UCL/HI rats treated with everolimus did not show significant hyperactive behaviors and social deficits in later life, suggesting an important role of activation of mTOR signaling pathway in inducing autism-like behavior following early life HI insult.

Everolimus readily crosses the blood-brain-barrier (BBB), and was reported to yield higher brain concentrations in young compared to adult rats (7). These concentration variances are attributed in part to lower expression in young rats of P-glycoprotein (P-gp), an active efflux transporter and critical component of BBB (7). Although young age of rats and low P-gp expression may subsequently lead to greater negative effects of everolimus on brain metabolism than in adult rats, we have found everolimus to be well tolerated at doses applied in our experiments. The results presented here also suggest that everolimus may be protective after neonatal hypoxic-ischemic brain injury and in EOP.

Our gait analysis has shown significant left side-right side motoric differences in the hind paws of UCL/HI animals when compared to normoxic controls, a finding consistent with HI-induced brain injury. Importantly, in the everolimus treated UCL/HI animals gait defects were markedly reduced compared to untreated rats, although subtle left side-right side differences were still observed for some of the tested parameters.

CONCLUSIONS

The results of our experiments on an animal model of EOP presented here show overexpression of CBS and mTOR signaling components in the rat brain as early as 24 h after UCL/HI that last well into rat young age. Likewise, these animals have exhibited altered socialization, a behavioral hallmark of ASD, and hyperactivity in addition to motor deficits in later life. Our results also demonstrate feasibility of prevention/reversal of neurocognitive and motor consequences of neonatal hypoxic-ischemic brain injury by pharmacological blockade of mTOR, administered solely after the insult. These findings thus offer a potential new target for treatment of EOP, presently still an untreatable cause of autism, hyperactivity and cerebral palsy.

DECLARATION OF CONFLICTING INTERESTS

The authors declare that they have no conflicting interests.

FUNDING

This work was supported by a research grant awarded by the Zimin Foundation to the University of California, Davis (PI: ML) and the New York University (PIs: EN and DZ).

ETHICAL APPROVAL

The vertebrate animal protocol used in this study was approved by an Institutional Animal Care and Use Committee (IACUC) at the University of California, Davis (protocol number: 17420).

REFERENCES

1. Azmitia EC, Saccomano ZT, Alzoobaee MF, Boldrini M, Whitaker-Azmitia PM (2016) Persistent angiogenesis in the autism brain: an immunocytochemical study of postmortem cortex, brainstem and cerebellum. *J Autism Dev Disord* **46**:1307–1318.
2. Berman RF, Willemsen R (2009) Mouse models of fragile X-associated tremor ataxia. *J Investig Med* **57**:837–841.
3. Chan SJ, Chai C, Lim TW, Yamamoto M, Lo EH, Lai MK, Wong PT (2015) Cystathionine β-synthase inhibition is a potential therapeutic approach to treatment of ischemic injury. *ASN Neuro* **7**:1–14.
4. Coletta C, Papapetropoulos A, Erdelyi K, Olah G, Módis K, Panopoulos P *et al* (2012) Hydrogen sulfide and nitric oxide are mutually dependent in the regulation of angiogenesis and endothelium-dependent vasorelaxation. *Proc Natl Acad Sci U S A* **109**:9161–9166.
5. Crawley JN (2004) Designing mouse behavioral tasks relevant to autistic-like behaviors. *Ment Retard Dev Disabil Res Rev* **10**:248–258.
6. Franz DN, Belousova E, Sparagana S, Bebin EM, Frost M, Kuperman R *et al* (2013) Efficacy and safety of everolimus for subependymal giant cell astrocytomas associated with tuberous sclerosis complex (EXIST-1): a multicentre, randomised, placebo-controlled phase 3 trial. *Lancet* **381**:125–132.
7. Gottschalk S, Cummins CL, Leibfritz D, Christians U, Benet LZ, Serkova NJ (2011) Age and sex differences in the effects of the immunosuppressants cyclosporine, sirolimus and everolimus on rat brain metabolism. *Neurotoxicology* **32**:50–57.
8. Haynes RL, Folkerth RD, Keefe RJ, Sung I, Swzeda LI, Rosenberg PA *et al* (2003) Nitrosative and oxidative injury to premyelinating oligodendrocytes in periventricular leukomalacia. *J Neuropathol Exp Neurol* **62**:441–450.
9. Hoeffer CA, Klann E (2010) mTOR signaling: at the crossroads of plasticity, memory and disease. *Trends Neurosci* **33**:67–75.

10. Hütt-Cabezas M, Karajannis MA, Zagzag D, Shah S, Horkayne-Szakaly I, Rushing EJ *et al* (2013) Activation of mTORC1/mTORC2 signaling in pediatric low-grade glioma and pilocytic astrocytoma reveals mTOR as a therapeutic target. *Neuro Oncol* **15**:1604–1614.
11. Jantzie LL, Talos DM, Jackson MC, Park HK, Graham DA, Lechpammer M *et al* (2015) Developmental expression of N-methyl-D-aspartate (NMDA) receptor subunits in human white and gray matter: potential mechanism of increased vulnerability in the immature brain. *Cereb Cortex* **25**:482–495.
12. Kim E, Camacho J, Combs Z, Ariza J, Lechpammer M, Noctor SC, Martínez-Cerdeño V (2015) Preliminary findings suggest the number and volume of supragranular and infragranular pyramidal neurons are similar in the anterior superior temporal area of control subjects and subjects with autism. *Neurosci Lett* **589**:98–103.
13. Kimura H (2000) Hydrogen sulfide induces cyclic AMP and modulates the NMDA receptor. *Biochem Biophys Res Commun* **267**:129–133.
14. Land SC, Tee AR (2007) Hypoxia-inducible factor 1alpha is regulated by the mammalian target of rapamycin (mTOR) via an mTOR signaling motif. *J Biol Chem* **282**:20534–20543.
15. Lechpammer M, Manning SM, Samonte F, Nelligan J, Sabo E, Talos DM *et al* (2008) Minocycline treatment following hypoxic/ischaemic injury attenuates white matter injury in a rodent model of periventricular leucomalacia. *Neuropathol Appl Neurobiol* **34**:379–393.
16. Lechpammer M, Wintermark P, Merry KM, Jackson MC, Jantzie LL, Jensen FE (2016) Dysregulation of FMRP/mTOR signaling cascade in hypoxic-ischemic injury of premature human brain. *J Child Neurol* **31**: 426–432.
17. Liu X, Pan L, Zhuo Y, Gong Q, Rose P, Zhu Y (2010) Hypoxia-inducible factor-1α is involved in the pro-angiogenic effect of hydrogen sulfide under hypoxic stress. *Biol Pharm Bull* **33**:1550–1554.
18. Liu Y, Zou LP, Jun-Bao Du JB, Wong V (2010) Electro-acupuncture protects against hypoxic–ischemic brain-damaged immature rat via hydrogen sulfide as a possible mediator. *Neuroscience* **485**:74–78.
19. Luhachack L, Nudler E (2014) Bacterial gasotransmitters: an innate defense against antibiotics. *Curr Opin Microbiol* **21**:13–17.
20. Moy SS, Nadler JJ, Perez A, Barbaro RP, Johns JM, Magnuson TR *et al* (2004) Sociability and preference for social novelty in five inbred strains: an approach to assess autistic-like behavior in mice. *Genes Brain Behav* **3**:287–302.
21. Parasuraman S (2011) Toxicological screening. *J Pharmacol Pharmacother* **2**:74–79.
22. Qu K, Chen CP, Halliwell B, Moore PK, Wong PT (2006) Hydrogen sulfide is a mediator of cerebral ischemic damage. *Stroke* **37**:889–893.
23. Schmitt U, Hiemke C (1998) Combination of open field and elevated plus-maze: a suitable test battery to assess strain as well as treatment differences in rat behavior. *Prog Neuropsychopharmacol Biol Psychiatry* **22**:1197–1215.
24. Shaikh H, Lechpammer M, Jensen FE, Warfield SK, Hansen AH, Kosaras B *et al* (2015) Increased brain perfusion persists over the first month of life in term asphyxiated newborns treated with hypothermia: Does it reflect activated angiogenesis? *Transl Stroke Res* **6**:224–233.
25. Shao JL, Wan XH, Chen Y, Bi C, Chen HM, Zhong Y *et al* (2011) H_2S protects hippocampal neurons from anoxia–reoxygenation through cAMP-mediated PI3K/Akt/p70S6K cell-survival signaling pathways. *J Mol Neurosci* **43**:453–460.
26. Slivka A, Cohen G (1993) Brain ischemia markedly elevates levels of the neurotoxic amino acid, cysteine. *Brain Res* **608**:33–37.
27. Szabo C (2007) Hydrogen sulphide and its therapeutic potential. *Nat Rev Drug Discov* **6**:917–935.
28. Takei N, Nawa H (2014) mTOR signaling and its roles in normal and abnormal brain development. *Front Mol Neurosci* **7**:28.
29. Vandeputte C, Taymans JM, Casteels C, Coun F, Ni Y, Van Laere K, Baekelandt V (2010) Automated quantitative gait analysis in animal models of movement disorders. *BMC Neurosci* **11**:92.
30. Volpe JJ (2009) The encephalopathy of prematurity–brain injury and impaired brain development inextricably intertwined. *Semin Pediatr Neurol* **16**:167–178.
31. Wang JF, Li Y, Song JN, Pang HG (2014) Role of hydrogen sulfide in secondary neuronal injury. *Neurochem Int* **64**:37–47.
32. White SW, Oswald D, Ollendick T, Scahill L (2009) Anxiety in children and adolescents with autism spectrum disorders. *Clin Psychol Rev* **29**:216–229.
33. Wong PT, Qu K, Chimon GN, Seah AB, Chang HM, Wong MC *et al* (2006) High plasma cyst(e)ine level may indicate poor clinical outcome in patients with acute stroke: possible involvement of hydrogen sulfide. *J Neuropathol Exp Neurol* **65**:109–115.
34. Zagzag D, Capo V (2002) Angiogenesis in the central nervous system: a role for vascular endothelial growth factor/vascular permeability factor and tenascin-C. Common molecular effectors in cerebral neoplastic and non-neoplastic "angiogenic diseases". *Histol Histopathol* **17**:301–321.